

**Title: Sensitivity of UV Erythemal Radiation to Total Ozone  
Changes under Different Sky Conditions: Results for Granada,  
Spain**

**Author(s): Anton, M.; Cazorla, A.; Mateos, D.; M. J. Costa, F.J.**

**Olmo and L. Alados-Arboledas et al.**

**Source: Photochemistry and Photobiology**

**Volume: 92 Issue: 1 Pages: 215-219**

**Published: 2016**

**DOI: 10.1111/php.12539**

This is the peer reviewed version of the following article: Antón, M.; et al. Sensitivity of UV Erythemal Radiation to Total Ozone Changes under Different Sky Conditions: Results for Granada, Spain. Photochemistry and Photobiology, 92(1): 215-219 (2016), which has been published in final form at <http://dx.doi.org/10.1111/php.12539> . This article may be used for non-commercial purposes in accordance with Wiley Terms and Conditions for Self-Archiving

# **Sensitivity of UV erythemal radiation to total ozone changes under different sky conditions: results for Granada, Spain**

M. Antón<sup>1,2\*</sup>, A. Cazorla<sup>3,4</sup>, D. Mateos<sup>5</sup>, M. J. Costa<sup>2</sup>, F.J. Olmo<sup>3,4</sup> and L. Alados-Arboledas<sup>3,4</sup>

<sup>1</sup> Departamento de Física, Universidad de Extremadura, Badajoz, Spain

<sup>2</sup> Departamento de Física, Instituto de Ciências da Terra, Escola de Ciências e Tecnologia, Universidade de Évora, Évora, Portugal

<sup>3</sup> Instituto Interuniversitario del Sistema Tierra en Andalucía, Granada, Spain

<sup>4</sup> Departamento de Física Aplicada, Universidad de Granada, Granada, Spain

<sup>5</sup> Grupo de Óptica Atmosférica (GOA), Universidad de Valladolid, Valladolid, Spain

\*Corresponding author e-mail: [mananton@unex.es](mailto:mananton@unex.es) (Manuel Antón)

## ABSTRACT

This paper focuses on the analysis of the sensitivity of UV erythemal radiation (UVER) to variations of the total ozone column (TOC) under different sky conditions at Granada (southeastern Spain). The sensitivity is studied both in relative terms by means of the Radiation Amplification Factor (RAF) and in absolute terms using the Ozone Efficiency (OE). These two variables are determined for diverse sky conditions characterized by the cloud cover information given by a sky camera (in oktas) and the cloud optical depth (COD) estimated from global solar radiation measurements. As expected, in absolute terms, the TOC variations cause substantially smaller UVER changes during completely overcast situations than during cloud-free cases. For instance, the OE (SZA=30°, TOC=290 DU) decreases from 0.68 mW/m<sup>2</sup> per unit of TOC (0 oktas) to 0.50 mW/m<sup>2</sup> per unit of TOC (8 oktas). However, the opposite is observed when the analysis is performed in relative terms. Thus, the RAF (determined for SZA cases below 80°) increases from 1.1 for cloud-free cases (0 oktas) to 1.4 for completely overcast situations (8 oktas). This opposite behavior is also found when both RAF and OE are analyzed as functions of COD. Thus, while the OE strongly decreases with increasing COD, the RAF increases as COD increases.

## INTRODUCTION

There is currently a growing interest in evaluating the ultraviolet (UV) radiation levels at the Earth's surface due mainly to the potentially harmful effects of this radiation on human health, ecosystems, photochemical processes and materials (1). Among the adverse effects associated with UV radiation overexposure, the erythema or sunburn of human skin receives a notable attention by society. The UV erythemal radiation (UVER) accounts for this effect weighting the solar UV radiation with the erythemal spectral response function (2). This spectral response exhibits its maximum sensitivity in the UV-B spectral range (280-315 nm) where the ozone variations produce great radiative effects.

Diverse physical and photochemical processes of scattering and absorption attenuate UVER through the atmosphere, causing substantially smaller UVER values at the Earth's surface than at the top of the atmosphere. The atmospheric ozone is the main attenuating factor and its influence on UVER at the surface has been usually studied by means of the Radiation Amplification Factor (RAF) defined as the percentage increase in UVER that would result from a 1% decrease in the total ozone column (3). The RAF has become a widely used standard index during last decades to evaluate the UVER sensitivity to atmospheric ozone changes at different locations worldwide (4-8). RAF values are usually referred to cloud-free conditions due to the strong influence of cloudiness over the short-term variability of UVER data (9-11). Hence, RAF values for cloudy conditions are reported only in a few works in literature (12, 13).

In this framework, the main objective of this paper is to evaluate the sensitivity of UVER values to atmospheric ozone changes during different sky conditions at Granada (southeastern

Spain) both in relative terms from the RAF and in absolute terms by means of the Ozone Efficiency (UVER change per unit of ozone column). For this goal, the empirical expression proposed by Antón et al. (14) for all sky conditions is used together with cloud cover information given by a sky camera and cloud optical depth (COD) values estimated from global solar radiation measurements. It is therefore expected that this paper will improve the understanding of the impact of ozone changes on UV radiation.

## **MATERIALS AND METHODS**

*Datasets.* All data used in this paper were measured between January 2006 and December 2014 at the radiometric station located on the rooftop of the Andalusian Center for Environmental Studies (CEAMA, 37.16N, 3.58 W, 680 ma.s.l.) in Granada (southeastern Spain). This station is operated by the Atmospheric Physics Group (GFAT) of the Granada University.

UVER data were recorded every minute by a broadband UV radiometer, model UVB-1, manufactured by Yankee Environmental Systems, Inc. (Massachusetts, US). Output voltages were converted into UVER values applying the calibration factors derived from three calibration campaigns of broadband UV radiometers, which took place at the “El Arenosillo” INTA station in Huelva (Spain) in 2007, 2011 and 2013. These campaigns included the spectral and angular characterization of the UVB-1 radiometer and their absolute calibration, performed through the outdoor intercomparison with respect to a reference Brewer spectroradiometer (15).

Global solar irradiance (0.305-2.8  $\mu\text{m}$ ) was measured by a CM-11 pyranometer manufactured by Kipp & Zonen (Delft, The Netherlands), which was periodically checked against a reference pyranometer at the study site. From these measurements, COD data were estimated following the

expression proposed and tested by Barnard et al. (16) being adequate to characterize the influence of clouds on the UV spectral range (17). As suggested by the authors, a simple criteria based on cloud transmission values is adopted: when it is above 0.8 ice cloud properties are assumed in the COD evaluations, meanwhile values below 0.8 are an indicator of liquid water clouds. The uncertainty attributed to these COD retrievals was about 1 (16), and the use of this info as input in radiative transfer simulations to obtain spectral cloud transmissions in the UV range, compared to experimental data, provides an uncertainty below 12% for COD varying between 10 and 20 (17). The required cloud-free estimations in this methodology are empirically evaluated using only the entire cloud-free days available in the analyzed period (detected by the all-sky camera, see next paragraph). In addition, the clearness index ( $k_t$ ) was also obtained as the ratio of the global solar irradiance to the extraterrestrial global solar irradiance on a horizontal surface (18). Both COD and  $k_t$  values were obtained with 1-minute intervals during daytime.

An All-Sky Imager provided images of the whole sky dome during daytime at 5 min intervals. This instrument is a custom adaptation of a CCD camera using a digital color video camera mounted with a fish-eye lens (180 FOV) pointing to the zenith which provides cloud cover information in oktas (i.e., eighths of the sky obscured by clouds) (19, 20).

Daily values of the total ozone column (TOC) in Dobson Units (DU) over the study site were provided by the Ozone Monitoring Instrument (OMI) (21). The OMI satellite data used in this work were retrieved from the OMI-TOMS algorithm, which is based on the long-standing NASA TOMS V8 retrieval algorithm (22).

*Methodology.* Antón et al. (14) proposed the following analytic formula to relate UVER to TOC values for all-sky conditions:

$$UVER \sim a (\mu_0)^b (TOC)^c (k_t)^d \quad (1)$$

where  $\mu_0$  is the cosine of the solar zenith angle (SZA), and  $k_t$  is the clearness index which is derived from total solar irradiances recorded with the CM-11 pyranometer. The SZA is obtained for each sky image taken every 5 min, the 1-min UVER and  $k_t$  data were averaged within  $\pm 1$  min of each sky image (three 1-min measurements), while TOC corresponded to daily OMI observations. The coefficient  $c$  is a useful indicator of the sensitivity of UVER to variation in TOC, representing the negative value of the RAF (23).

The expression 1 is based on the multiplicatively separate power dependences of UVER on both  $\mu_0$  and TOC values, which was explained in detail by Micheletti et al. (24) and subsequently used by Madronich (23) to estimate the UV Index (UVI) data for cloud-free and unpolluted cases. Anton et al. (14) proposed a more general expression (Eq. 1) which accounts for the possible presence of clouds and aerosols via the clearness index.

Another relevant magnitude to analyze the sensitivity of UVER values to TOC changes is the Ozone Efficiency (OE), defined as the rate at which the UVER is “forced” per unit of TOC, being expressed as follows (25):

$$OE = \frac{dUVER}{dTOC} \quad (2)$$

Therefore, the OE for all-sky conditions can be calculated performing the derivate of Eq. 1 with respect to TOC:

$$OE \sim c \cdot a (\mu_0)^b (TOC)^{c-1} (k_t)^d \quad (3)$$

While the RAF reports about the relative UVER changes due to relative TOC changes, the OE reports about the relationship between the absolute variations (in physical units) in UVER and

TOC values. As the coefficient  $c$  has negative sign, OE also presents a negative value which indicates that an increase (decrease) of TOC produces a decrease (increase) of UVER.

Nevertheless, in this study, the OE values are shown with positive sign like the RAF values.

## **RESULTS AND DISCUSSION**

With the purpose of analyzing in detail the cloudiness influence on the sensitivity of UVER values to ozone changes, the RAF was determined for sky conditions with identical cloud cover using UVER,  $\mu_0$ ,  $k_t$  and TOC data for those cases with SZA below  $80^\circ$ . For this goal, a multiple regression analysis (Eq. 1) was performed using the least squares approach for each fraction of cloud cover measured by the All-Sky Imager. Taking the natural logarithm of Eq. 1 provides a linear equation in  $\ln(\mu_0)$ ,  $\ln(\text{TOC})$ ,  $\ln(k_t)$  and with regression coefficients  $b$ ,  $c$  and  $d$ . We then define a confidence limit of 95% for the regression and resultant coefficients. Table 1 shows RAF values with their intervals at the 95% level of confidence for each cloud cover (in oktas), including the number of data used in each regression analysis and two statistical parameters: the coefficient of determination ( $R^2$ ) and the root mean square error (RMSE). The regression analysis shows excellent results with  $R^2$  higher than 0.97 for all cloud cover cases and RMSE smaller than 15% for cloud cover below 6 oktas. This latter statistical parameter reaches a value of 26% for almost overcast conditions (7 oktas) and 37% for completely overcast situations (8 oktas), which indicate a notable increase of the spread for these cloudy cases. Regarding the RAF, Table 1 displays similar values around 1.1 both for cloud-free conditions (0 oktas) and for partially cloudy conditions ( $1 \leq \text{oktas} \leq 5$ ). These RAF values are in accordance with the experimental results reported by several studies for cloud-free cases (3,



5). Above 5 oktas, the RAF increases its value with increasing cloud cover up to 1.44 for completely overcast conditions (8 oktas). This dependence on cloud cover is statistically significant since the intervals of confidence do not overlap for the RAF values corresponding to cloud cover between 5 and 8 oktas. Additionally, a RAF of 1.17 is obtained when the regression analysis is performed using all available data (all sky conditions), close to the RAF values for fractions of cloud cover smaller than 5 oktas but substantially smaller than the RAF for completely overcast conditions. This result can be related to the large number of cases with cloud cover between 0 and 5 oktas (71% of all cases). Thus, the weighted mean of the RAF values for the nine fractions of cloud cover taking into account the number of cases for each fraction is 1.16. Hence, the RAF derived from data recorded during all-sky conditions can notably differ if the study site is mainly affected by cloud-free or cloudy conditions.

From the results commented above, if there is a relative decrease of 1% in the TOC between two overcast cases with the same SZA and  $k_t$ , then UVER increases around 1.4% in Granada site, while an identical relative TOC decrease during cloud-free conditions produces an UVER increase of around 1.1%. Hence, in relative terms, UVER exhibits a larger sensitivity to ozone changes during overcast conditions than during cloud-free situations. This behavior is mainly due to the shift that clouds cause toward shorter wavelengths where the UVER sensitivity to ozone changes is higher (26). This shift occurs because under clear sky conditions the shorter wavelengths are already attenuated by Rayleigh scattering more than the longer wavelengths and, so the clouds will overwhelm this Rayleigh-induced wavelength dependence. Furthermore, the clouds increase the upward flux of photons above them, being some of those photons backscattered in the downward direction through Rayleigh scattering with the subsequent increase of downward flux at the cloud top (27). Additionally, the

tropospheric ozone located within clouds may also produce an amplification of UV absorption due to the enhancement in the optical path by scattering processes (28-30). These phenomena explain that any ozone variation during cloudy conditions will cause a larger radiative amplification, in relative terms, than during the equivalent cloud-free cases.

One should bear in mind that RAF informs about relative changes in both UVER and TOC, so the larger RAF values observed for overcast cases than for cloud-free conditions do not imply that the ozone depletion episodes in heavy cloudy days will have a stronger erythemal effect than the same ozone depletion event in cloud-free days. To analyze this issue, the OE quantifies the absolute UVER changes per unit of TOC, being dependent on the SZA, TOC, and sky conditions. OE values were obtained from the full expression given by Eq. 3 for each sky image taken every 5 min for all SZA below 80°. The coefficients (a, b, c and d) used in Eq. 3 to obtain the OE values were determined for each fraction of cloud cover from the multiple regression analysis given by Eq. 1. Table 2 shows the OE averages ( $\pm$  one standard deviation) for each fraction of cloud cover and four specific cases with fixed SZA and TOC values. It can be seen that that OE values are substantially smaller for SZA=60° than for SZA=30° due to the strong decrease of UVER with increasing SZA under similar TOC and cloud cover conditions. Furthermore, for a fixed SZA and cloud cover, OE is higher for a TOC of 290 DU than for 350 DU because, as ozone decreases, the UVER values recorded at surface are larger. Regarding the influence of sky conditions on OE values, Table 2 shows that, for each of the four selected cases, the OE displays similar values below 6 oktas, while this variable substantially reduces its value for those cloudy cases with 7 and 8 oktas. For instance, the OE (SZA=30°, TOC=290 DU) exhibits values between 0.62 and 0.68 mW/m<sup>2</sup> per DU for cloud covers below 6 oktas, decreasing up to 0.53 and 0.50 mW/m<sup>2</sup> per DU for cloud cover

cases with 7 and 8 oktas, respectively. Therefore, as expected, the absolute TOC changes during overcast conditions produce notably smaller absolute variations of UVER values than during cloud-free cases.

The results summarized in Tables 1 and 2 show that the fraction of cloud cover notably affects the sensitivity of UVER values due to ozone changes. Nevertheless, sky conditions with identical cloud cover may present different optical characteristics. The COD or equivalently, column integrated extinction in the cloudy system, is the crucial cloud property determining the solar radiation at the Earth's surface (31). Therefore, it will be highly interesting to analyze the impact of COD variations on both the RAF and OE values. For that purpose, multiple regression analyses given by Eq. 1 have been performed for 20 intervals of COD using bins of 5 from 0-5 to 95-100. These COD data were derived from solar radiation measurements recorded exclusively during overcast conditions (8 oktas) when the accuracy of COD estimations is ensured (16, 17, 30). Regarding the type of clouds analyzed for these overcast situations, ceilometer measurements indicate that 81% of the cloudy cases considered during 2013 and 2014 correspond to water clouds (cloud top heights below 5 km). The cloud phase retrievals from MODIS cloud product Level 2 data (collection 6) were also checked for the selected overcast cases. As a result, 70% of MODIS retrievals correspond to liquid phase.

Figure 1 shows the RAF (determined for SZA cases below  $80^\circ$ ) as a function of COD, where the error bars correspond to the intervals at the 95% level of confidence. Additionally, the OE (SZA= $60 \pm 1^\circ$ , TOC= $290 \pm 5$  DU) averaged for each COD bin has been also plotted, where errors bars is one standard deviation. It can be seen that the RAF clearly increases its value as COD increases from 1.2 for COD below 5 up to nearly 2 for COD above 90. Thus, the cloud

optical properties strongly affect the radiative amplification associated with the ozone changes. Clouds with large optical thickness likely lead to a shift toward shorter wavelengths than those clouds with small optical thickness, contributing to obtain larger RAF values. In contrast to the pattern observed for the RAF, the OE decreases approximately exponentially as the COD increases, roughly from 0.14 mW/m<sup>2</sup> per DU for COD below 5, to values smaller than 0.04 mW/m<sup>2</sup> per DU for COD above 50. This behavior evidences that, in absolute terms, the UVER variations due to TOC changes during overcast conditions are very sensitive to the COD values below 50. From this value of optical thickness on, the OE exhibits small values below 0.04 mW/m<sup>2</sup> per DU, since most of the radiation is reflected to space by the thick clouds (nearly opaque), and the UVER reaching the surface is mostly diffuse and isotropic (32), thus less affected, in absolute terms, by any TOC change.

## **CONCLUSION**

From the results obtained in this study, it can be stated that the analysis of the sensitivity of UVER values to TOC changes during different sky conditions differs if the analysis is performed in relative terms (from the RAF) or in absolute terms (from the OE). Thus, the RAF increases from 1.1 (0 oktas) to 1.4 (8 oktas), pointing out that, in relative term, the ozone changes produce larger UVER variations at surface during completely overcast conditions than during cloud-free cases. By contrast, in absolute term, as clouds usually produce a strong attenuation of the surface UVER values, their sensitivity to TOC changes during cloudy situations is substantially smaller than during cloudless cases. Additionally, both RAF and OE exhibit a great dependence on the cloud optical depth during overcast conditions, but with

opposite sign: while RAF increases with increasing COD, the OE substantially reduces its value as COD increases. To sum up, the UVER sensitivity to ozone changes is strongly affected by the sky conditions related to the cloud cover. Further investigation is needed in order to determine this sensitivity in other sites (e.g., urban areas with high aerosol load in the boundary layer).

**ACKNOWLEDGMENTS:** The authors thank the OMI team for the total ozone data used in this paper. Manuel Antón thanks Ministerio de Ciencia e Innovación and Fondo Social Europeo for the award of a postdoctoral grant (Ramon y Cajal). This work was supported by the Andalusia Regional Government through projects P10-RNM-6299 and P12-RNM-2409, by the Spanish Ministry of Economy and Competitiveness through projects CGL2011-29921-C02-01, CGL2013-45410-R, CGL2014-56255-C2-1-R, by European Commission Horizon 2020 Research and Innovation Framework Programme through ACTRIS 2 project (H2020-INFRAIA-2014-2015-654109) and by ICT, under contract with FCT (the Portuguese Science and Technology Foundation).

## **REFERENCES**

1. UNEP (2015), Environmental effects of ozone depletion and its interactions with climate change: 2014 Assessment, United Nations Environment Programme (UNEP), ISBN 978-9966-076-04-5, Nairobi, Kenya.
2. McKinlay, A. F., and B. L. Diffey (1987) A reference spectrum for ultraviolet induced

erythema in human skin. *CIE Journal*. **6**, 21-27.

3. McKenzie, R., W. Matthews, and P. Johnston (1991) The relationship between erythemal UV and ozone derived from spectral irradiance measurements. *Geophys. Res. Lett.* **18**, 2269-2272.

4. Bodhaine, B., E. Dutton, D. Hofmann, R. McKenzie, and P. Johnston (1997) UV measurements at Mauna Loa: July 1995 to July 1996. *J. Geophys. Res.* **102**, 19265-19273.

5. Madronich, S., R. McKenzie, R. Bjorn, and M. Caldwell (1998) Changes in biologically active ultraviolet radiation reaching the Earth's surface. *J. Photoch. Photobio. B* **46**, 5-19.

6. Dubrovsky, M. (2000) Analysis of UV-B irradiances measured simultaneously at two stations in the Czech Republic. *J. Geophys. Res.* **105**, 4907-4913.

7. Zerefos, C. (2002) Long-term ozone and UV variations at Thessalonika, Greece. *Phys. Chem. Earth* **27**, 455-460.

8. Herman, J.R., (2010) Use of an improved radiation amplification factor to estimate the effect of total ozone changes on action spectrum weighted irradiances and an instrument response function. *J. Geophys. Res.* **115**, D23119.

9. Calbó, J., D. Pagés, and J. González (2005) Empirical studies of cloud effects on UV radiation: A review. *Rev. Geophys.* **43**, doi:10.1029/2004RG000155.

10. Antón, M., J.E. Gil, A. Cazorla, J. Fernández-Gálvez, I. Foyo-Moreno, F.J. Olmo, and L. Alados-Arboledas (2011) Short-term variability of experimental ultraviolet and total solar irradiance in Southeastern Spain. *Atmos. Environ.* **45**, 4815-4821.

11. Aun, M., K. Eerme, I. Ansko, U. Veismann and S. Laätt (2011) Modification of spectral ultraviolet doses by different types of overcast cloudiness and atmospheric aerosol. *Photoch. Photobio.* **87**, 461-469.

12. den Outer, P.N., H. Slaper, and R. B. Tax (2005) UV radiation in the Netherlands: Assessing long-term variability and trends in relation to ozone and clouds. *J. Geophys. Res.* **110**, D02203, doi:10.1029/2004JD004824.
13. Kim, J., H. K. Cho, J. Mok, H. D. Yoo, and N. Cho (2013) Effects of ozone and aerosol on surface UV radiation variability. *J. Photoch. Photobio. B* **119**, 46-51.
14. Antón, M., A. Serrano, M.L. Cancillo, J.A. García and S. Madronich (2011) Empirical evaluation of a simple analytical formula for the Ultraviolet Index. *Photoch. Photobio.* **87**, 478-482.
15. Vilaplana, J.M., A. Serrano, M. Antón, M.L. Cancillo, M. Parias, J. Gröbner, G. Hulsen, G. Zablocky, A. Díaz, and B. de la Morena (2009) Report of the El Arenosillo/INTA-COST calibration an intercomparison campaign of UVER broadband radiometers, in: “El Arenosillo”, Huelva, Spain, August–September 2007, COST Office, ISBN:978-84-692-2640-7.
16. Barnard, J.C., C.N. Long, E.I. Kassianov, S.A. McFarlane, J.M. Comstock, M. Freer and G.M. McFarquhar (2008) Development and evaluation of a simple algorithm to find cloud optical depth with emphasis on thin ice clouds. *Open Atmos. Sci. J.* **2**, 46-55.
17. Mateos, D., A. di Sarra, J. Bilbao, D. Meloni, G. Pace, A. de Miguel, and G. Casasanta (2015) Spectral attenuation of global and diffuse UV irradiance and actinic flux by clouds. *Q. J. R. Meteorol. Soc.* **141**, 109–113.
18. Alados-Arboledas, L., F. J. Olmo, I. Alados, and M. Pérez (2000) Parametric models to estimate photosynthetically active radiation in Spain. *Agric. For. Meteorol.* **101**, 187-201.
19. Cazorla, A., F.J. Olmo, and L. Alados-Arboledas (2008) Development of a sky imager for cloud cover assessment. *J. Opt. Soc. Am. A.* **25**, 29–39.
20. Cazorla, A., F.J. Olmo, and L. Alados-Arboledas (2008) Using a sky imager for aerosol

- characterization. *Atmos. Environ.* **42**, 2739-2745.
21. Levelt, P. F., E. Hilsenrath, G. W. Leppelmeier, G. H. J. Van den Oord, P. K. Bhartia, J. Tamminen, J. F. De Haan, and J. P. Veefkind (2006) The ozone monitoring instrument. *IEEE Trans. Geosci. Remote Sens.* **44**, 1093–1101.
22. Bhartia, P. K., and C. Wellemeyer (2002) TOMS-V8 total O<sub>3</sub> algorithm, in OMI Algorithm Theoretical Basis Document, vol. II, OMI Ozone Products, edited by P. K. Bhartia, pp. 15– 31, NASA Goddard Space Flight Cent., Greenbelt, Md. (Available at <http://eospsso.gsfc.nasa.gov/sites/default/files/atbd/ATBD-OMI-02.pdf>).
23. Madronich, S. (2007) Analytic Formula for the Clear-sky UV Index. *Photochem. Photobiol.* **83**, 1537-1538.
24. Micheletti, M.I., R.D. Piacentini, S. Madronich (2003) Sensitivity of biologically active UV radiation to stratospheric ozone changes: Effects of action spectrum shape. *Photochem. Photobiol.* **78**, 456–461.
25. Antón, D. Mateos, R. Román, A. Valenzuela, L. Alados-Arboledas, and F. J. Olmo (2014) A method to determine the ozone radiative forcing in the ultraviolet range from experimental data. *J. Geophys. Res.* **119**, 1860-1873.
26. Seckmeyer, G., R. Erb, and A. Albold (1996) Transmittance of a cloud is wavelength-dependent in the UV-Range. *Geophys. Res. Lett.* **23**, 2753-2755.
27. Kylling, A., A. Albold, and G. Seckmeyer (1997) Transmittance of a cloud is wavelength-dependent in the UV-range: Physical interpretation. *Geophys. Res. Lett.* **24**, 397400.
28. Wang, P., and J. Lenoble (1996) Influence of clouds on UV irradiance at ground level and backscattered exittance. *Adv. Atmos. Sci.* **13**, 217-228.
29. Mayer, B., A. Kylling, S. Madronich, and G. Seckmeyer (1998) Enhanced absorption of



UV radiation due to multiple scattering in clouds, Experimental evidence and theoretical explanation. *J. Geophys. Res.* **103**, 31241-31254.

30. Mateos, D., A. di Sarra, D. Meloni, C. Di Biagio, and D. M. Sferlazzo (2011) Experimental determination of cloud influence on the spectral UV irradiance and implications for biological effects. *J. Atmos. Sol.-Terr. Phy.* **73**, 1739-1746.

31. Antón, M., L. Alados-Arboledas, J.L. Guerrero-Rascado, M.J. Costa, J. C Chiu, and F. J. Olmo (2012) Experimental and modeled UV erythemal irradiance under overcast conditions: the role of cloud optical depth. *Atmos. Chem. Phys.* **12**, 11723–11732.

32. Salgueiro, V., M.J. Costa, A.M. Silva, and D. Bortoli (2014) Variability of the daily-mean shortwave cloud radiative forcing at the surface at a midlatitude site in Southwestern Europe. *J. Clim.* **27**, 7769-7780.

## **TABLES**

**Table 1.** Results of the multiple regression analysis (Eq. 1) for each fraction of cloud-cover (in oktas) and all cases using SZA values below 80°. The parameters are the following: the RAF with their intervals at the 95% level of confidence; the number of data used in the regression analysis, N; coefficient of determination, R<sup>2</sup>; and the root mean square errors, RMSE.

Cloud-cover (oktas)	RAF	N	R <sup>2</sup>	RMSE (%)
0	1.084±0.004	112578	0.997	6.0
1	1.055±0.008	36242	0.996	6.6
2	1.026±0.012	18620	0.995	8.0
3	1.049±0.017	14997	0.992	10.3
4	1.059±0.021	12588	0.989	12.3
5	1.115±0.021	12291	0.989	12.9
6	1.228±0.021	13961	0.987	14.7
7	1.338±0.018	31063	0.973	25.6
8	1.438±0.019	39607	0.971	36.8
All cases	1.166±0.006	291947	0.984	20.2

**Table 2.** Ozone efficiency averages ( $\pm$ one standard deviation) from Eq. 3 for each fraction of cloud-cover (in oktas) and four specific cases with fixed SZA and TOC values.

Cloud-cover (oktas)	OE (mW/m <sup>2</sup> DU <sup>-1</sup> ) SZA=(30±1) <sup>o</sup> TOC= (290±5) DU	OE (mW/m <sup>2</sup> DU <sup>-1</sup> ) SZA=(30±1) <sup>o</sup> TOC= (350±5) DU	OE (mW/m <sup>2</sup> DU <sup>-1</sup> ) SZA=(60±1) <sup>o</sup> TOC= (290±5) DU	OE (mW/m <sup>2</sup> DU <sup>-1</sup> ) SZA=(60±1) <sup>o</sup> TOC= (350±5) DU

0	0.68±0.03	0.48±0.01	0.18±0.01	0.12±0.01
1	0.66±0.02	0.48±0.02	0.17±0.01	0.11±0.01
2	0.64±0.02	0.44±0.03	0.16±0.01	0.11±0.01
3	0.63±0.02	0.43±0.05	0.16±0.02	0.10±0.02
4	0.62±0.04	0.40±0.08	0.16±0.02	0.10±0.02
5	0.64±0.07	0.43±0.08	0.17±0.02	0.11±0.02
6	0.65±0.10	0.39±0.08	0.16±0.03	0.10±0.02
7	0.53±0.10	0.29±0.10	0.14±0.04	0.09±0.03
8	0.50±0.15	0.27±0.11	0.10±0.06	0.05±0.03
All cases	0.62±0.09	0.42±0.13	0.17±0.05	0.10±0.04

## FIGURES

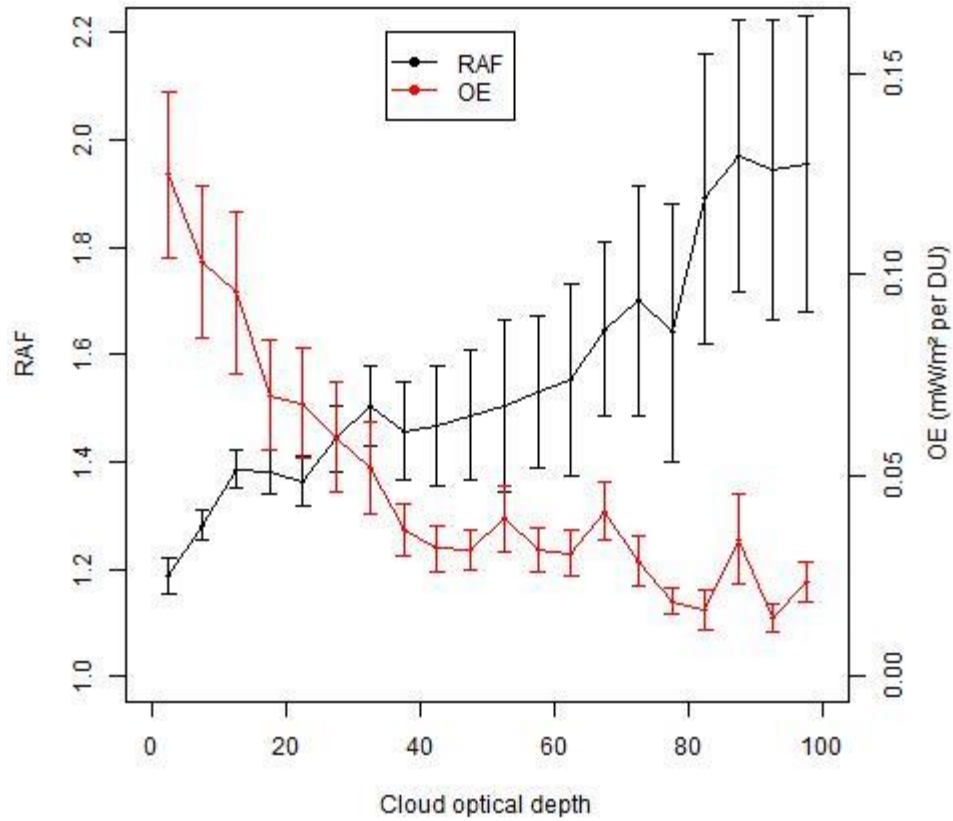


**Figure 1.** The RAF (determined for SZA cases below  $80^\circ$  from Eq. 1) and OE (determined for  $SZA=60\pm 1^\circ$  and  $TOC=290\pm 5$  DU from Eq. 3) as a function of COD using bins of 5 from 0-5 to 95-100 for overcast cloudy conditions (8 oktas).